2008 IEEE International Conference on
Robotics and Automation
Pasadena, CA, USA, May 19-23, 2008

Off-Road Robot Modeling with Dextrous Manipulation Kinematics

Joseph Auchter and Carl A. Moore

Abstract— **We present a novel way of modeling wheeled vehicles on outdoor terrains. Adapting concepts from dextrous manipulation, we precisely model the way that three dimensional wheels roll over uneven ground. The techniques used are easily adaptable to other vehicle designs of arbitrary complexity. Our modeling method is used to validate a new concept for design of off-road vehicle wheel suspensions, called Passive Variable Camber (PVC). Simulation results of a three-wheeled vehicle with PVC demonstrate that the vehicle can negotiate an extreme terrain without kinematic slip, thus improving vehicle efficiency and performance.**

I. INTRODUCTION

In recent years there has been increased interest in robots operating outdoors in unstructured environments [16],[6]. Despite this, the methods used to model mobile robots have not changed much. Traditional wheeled mobile robot (WMR) kinematic modeling (for example, [1]) assumes the robot moves on a planar surface. The wheels are modeled as thin disks and the velocity of each wheel center calculated by $v = \omega R$. As a result of these assumptions, non-holonomic constraints (such as enforcing rolling without slip at the wheel/ground contacts) are simple trigonometric relationships.

For outdoor WMRs the kinematic modeling process becomes very complex, mainly because the robot is now moving in a three-dimensional world instead of a two-dimensional one. On uneven terrain the contact point can vary along the surface of the wheel in both lateral and longitudinal directions. Therefore the motion of the wheel/ground contact points becomes complex. There is a need for an accurate model of this motion in order to properly study outdoor robots.

A. Previous Work

There have been several recent efforts to model the kinematic motion of WMRs on uneven terrains. However, none of them provide a complete model for the motion of the wheel/ground contact point due to rolling over the uneven ground. Capturing this motion precisely is of utmost importance when studying wheel slip, power efficiency, climbing ability, and path planning for outdoor robots.

Tarokh et al [15] provide a detailed kinematic model for the Rocky 7 Mars rover, but assume a 2-D wheel and do not provide a model for how the contact point moves along the surface of the wheel as it rolls on an uneven ground. Meghdari et al [9] develop a similar kinematic model for their CEDRA robot. However, they assume that certain characteristics of the wheel motion on the terrain are known without providing any equations describing the motion. The kinematic model of Tai [14] places a coordinate frame at the wheel/ground contact point, but no explanation is provided as to where the contact point is or how the motion is influenced by the terrain shape. Grand et al [3] perform a velocity analysis on their hybrid wheel-legged robot Hylos. They identify the contact point for each wheel and an associated frame, but make no mention of how these frames evolve as the vehicle moves.

B. Kinematic Slip

One of the problems associated with outdoor vehicles is wheel slip. In addition to dynamic slippage due to terrain deformation or insufficient friction, a WMR is affected by kinematic slip [2],[16]. Kinematic slip occurs when there is no instantaneous axis of rotation compatible with all of the robot's wheels. This is the general case on uneven terrain because the wheel/ground contact points vary along the surface of the wheel depending on the terrain shape and robot configuration. Ackermann steering geometry, designed to avoid such slip, works properly only on flat ground.

Wheel slip causes several problems. First, power is wasted [16],[2]. Second, wheel slip reduces the ability of the robot to self-localize because position estimates from wheel encoder data accumulate unbounded error over time [5]. Accurate kinematic models are needed to test robot designs which will potentially reduce this costly kinematic slip.

Sreenivasan and Nanua [13] used screw theory to explore the phenomenon of kinematic slip in wheeled vehicle systems moving on uneven terrain. Modeling two wheels joined by a rigid axle, their analysis showed that kinematic slip can be avoided if the distance between the wheel/ground contact points is allowed to vary. The authors of that work suggest the use of a Variable Length Axle (VLA) with a prismatic joint to achieve the necessary motion. The VLA is difficult to implement because it requires a complex wheel axle design.

As a more practical alternative to the VLA, Chakraborty and Ghosal [2] introduced the idea of adding an extra degree of freedom (DOF) at the wheel/axle joint, allowing the wheel to tilt laterally relative to the axle. This new capability, herein named Passive Variable Camber (PVC), permits the distance between the wheel/ground contact points to change without any prismatic joints. Figure 1 shows an example of an axle and two wheels equipped with PVC.

The authors would like to thank the NASA Faculty Awards for Research program for their generous support of research careers in science and engineering. Additional funding was provided by a university fellowship from the FSU Office of Graduate Studies.

Joseph Auchter (auchtjo@eng.fsu.edu) and Carl Moore (camoore@eng.fsu.edu) are with the Dept. of Mechanical Engineering, FAMU/FSU College of Engineering, Tallahassee, FL, USA.

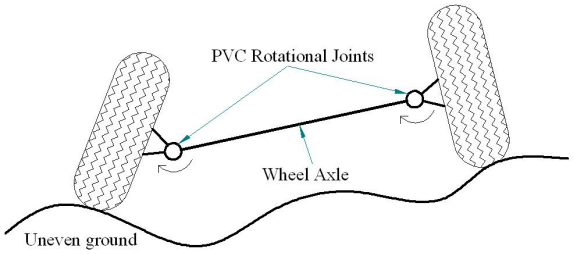

Fig. 1. Two tires on uneven ground attached to an axle equipped with Passive Variable Camber. The axis of rotation of each PVC joint is perpendicular to the page.

C. Contribution of this work

Traditional methods are not suitable for kinematic modeling of outdoor WMRs due to the complex nature of the terrain/robot system. More recent efforts to model outdoor vehicle motion lack convincing descriptions of how a realistic wheel rolls over an arbitrary uneven terrain.

In order to precisely model the way that three dimensional wheels roll over uneven ground, we adapt concepts developed for modeling dextrous robot manipulators. To our knowledge, the union of the worlds of WMR modeling and dextrous manipulator modeling is novel and does not suffer from many of the assumptions inherent in other modeling techniques. Also, our method is easily adaptable to other vehicle designs of arbitrary complexity.

This document introduces a kinematic simulation of a 3-wheeled mobile robot equipped with Passive Variable Camber and operating on uneven terrain. The purpose of the simulation is to verify that a WMR equipped with PVC can traverse uneven terrain without kinematic slip. Based on the results, PVC has the potential to improve the performance of robots moving on rough terrains.

II. Analogy Between WMRs and Dextrous Manipulators

In this work a kinematic model of the WMR/ground system is developed using techniques from the field of dextrous robot hands. The kinematics of dextrous manipulation provide an ideal description of the way wheels roll over uneven terrain.

A WMR in contact with uneven ground is analogous to a multi-fingered robotic "hand" (the WMR) grasping an "object" (the ground). The theories relating to manipulator contact and grasping are well-suited to modeling of outdoor vehicles. Table I summarizes the analogies between robotic hands and WMRs.

TABLE I
Relationships between manipulators and WMRs

Manipulators	Mobile Robots
Multi-fingered hand	Wheeled mobile robot
Grasped object	Ground
Fingers	Wheels
Palm	Robot platform

III. Wheeled Mobile Robot System with PVC

The modeling techniques described in this paper can be applied to any wheeled vehicle. In this section we illustrate our modeling techniques by using a representative example: a three-wheeled mobile robot (one front and two rear wheels). The front wheel is steerable, and the two rear wheels have PVC joints. The wheels are torus-shaped, which is more realistic than the typical thin-disk model [13].

A. Wheel/Ground Contact Model

Montana [10] was the first to develop kinematic contact equations which describe how two arbitrarily-shaped smooth surfaces roll/slide against each other. In our case the two surfaces are the wheel and ground. In this section we will develop the tools that we need in order to make use of the contact equations. For a good overview of dextrous manipulation and the associated mathematics, see [11].

The surface of each wheel is parameterized relative to its frame $\{W\}$ by u_i and v_i. This means that a unique point on the surface of the wheel (in the cartesian coordinates of $\{W_i\}$) is $f(u_i, v_i)$. Similarly, ground surface is parameterized relative to its frame $\{G\}$ by x and y. This means a unique point on the ground surface is $(x, y, g(x, y)) = (x, y, z)$.

Montana's equations describe the motion of the point of contact across the surfaces in response to a relative motion between the wheel and the ground. This motion has five degrees of freedom (DOFs). The only constraint is that contact must be maintained: no translational component of motion along their common surface normal is allowed. These five DOFs have the following interpretation: two DOFs each for the position of the contact point on the two surfaces (wheel and ground), and one DOF for rotation about the surface normal. The parameters that describe these five DOFs for wheel i are

$$\eta_i = [u_i \; v_i \; x_i \; y_i \; \psi_i]^T, \quad i = 1, 2, 3$$

where ψ_i is the angle of rotation about the common surface normal. They are grouped for all three wheels as: $\eta = [\eta_1^T \; \eta_2^T \; \eta_3^T]^T$.

Figures 2 and 3 show the coordinate frames which will be used to develop the kinematic equations. The frame definitions and other conventions follow [10]; see that work for more details. Frame $\{G\}$ is the ground reference frame. Frame $\{contG_i\}$ is the ground contact frame for wheel i. The z-axis of $\{contG_i\}$ is the outward normal to the ground surface at the contact point. Frame $\{P\}$ is the robot platform reference frame. $\{A_i\}$ is the frame at the point of attachment of the wheel i to the platform. $\{W_i\}$ is the reference frame of wheel i. $\{contW_i\}$ is the contact frame relative to wheel i. Its z-axis is the outward pointing normal from the torus-shaped wheel, which is collinear with the z-axis of $\{contG_i\}$. ψ_i is the angle between the x-axes of frames $\{contG_i\}$ and $\{contW_i\}$.

Also important are the velocities of the wheel relative to the ground:

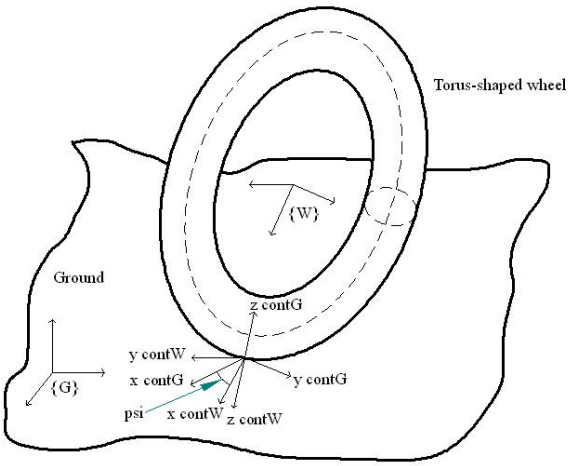

Fig. 2. Coordinate frames of the wheel and ground.

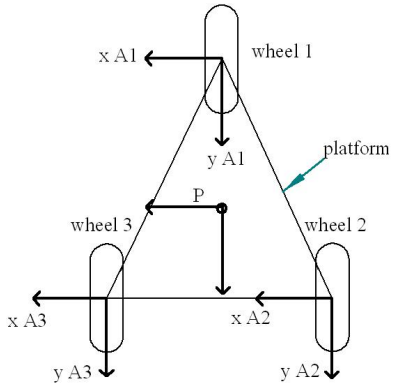

Fig. 3. Coordinate frames of the robot platform.

$$^{contW}V_{GW} = V_c = [v_x\ v_y\ v_z\ \omega_x\ \omega_y\ \omega_z]^T \tag{1}$$

The leading superscript indicates that the vector is resolved in the $\{contW\}$ frame. The trailing subscripts $\{GW\}$ indicate that the velocity is of frame $\{W\}$ relative to frame $\{G\}$. Since we are interested in enforcing rolling contact (no sliding), we define the "allowable contact velocities" as a subset of V_c:

$$\tilde{V}_c = [\omega_x\ \omega_y\ \omega_z]^T. \tag{2}$$

Montana [10] developed kinematic equations which describe how two arbitrarily-shaped smooth surfaces roll/slide against each other. In our case the two surfaces are the wheel and ground. Metric (M), curvature (K), and torsion (T) forms from differential geometry are used to describe the ground and wheel surfaces. The equations for rolling contact are:

$$\begin{aligned}(\dot{u},\dot{v})^T &= M_w^{-1}\left(K_w + K^*\right)^{-1}(-\omega_y,\omega_x)^T \\ (\dot{x},\dot{y})^T &= M_g^{-1}R_\psi\left(K_w + K^*\right)^{-1}(-\omega_y,\omega_x)^T \\ \dot{\psi} &= \omega_z + T_w M_w\,(\dot{u},\dot{v})^T + T_g M_g\,(\dot{x},\dot{y})^T.\end{aligned} \tag{3}$$

where subscript w indicates the wheel and g indicates the ground. See [10] for more details about these equations and their derivation. The inputs to these equations are the allowable contact velocities $\tilde{V}_c$, and the outputs are $\dot{\eta}$, so we abbreviate them by:

$$\dot{\eta} = [CK]\ \tilde{V}_c, \tag{4}$$

where $[CK]$ stands for "Contact Kinematics". These are the non-holonomic constraints of the robot/ground system.

B. Robot Configuration Variables

In this section we introduce the position and velocity variables which describe the state of the robot. The vector of joint velocities is:

$$\dot{\theta} = \left[\dot{\phi}_1\ \dot{\alpha}_1\ \dot{\gamma}_2\ \dot{\alpha}_2\ \dot{\gamma}_3\ \dot{\alpha}_3\right]^T$$

where $\dot{\alpha}_i$ is the driving rate of wheel i, $\dot{\phi}_1$ is the steering rate of wheel 1, $\dot{\gamma}_i$ is the rate of tilt of the wheel about the PVC joint of wheel i (for $i = 2, 3$).

The relative velocity between the ground and platform is V_{PG}. The vectors of configuration and velocity variables which define the state of the robot/ground system are grouped together as:

$$q = \begin{bmatrix}\theta\\ \eta\\ P_{PG}\\ \tilde{P}_c\end{bmatrix}, \quad \dot{q} = \begin{bmatrix}\dot{\theta}\\ \dot{\eta}\\ V_{PG}\\ \tilde{V}_c\end{bmatrix}, \tag{5}$$

where P_{PG} and $\tilde{P}_c$ are the position equivalents of V_{PG} and $\tilde{V}_c$, respectively.

IV. Kinematic Modeling Method

In this section, our method for kinematic modeling of the three-wheeled mobile robot is introduced. Table II shows the desired inputs and outputs for the forward kinematics.

TABLE II
FORWARD KINEMATICS INPUTS AND OUTPUTS

Inputs	Outputs
Desired wheel joint velocities $\dot{\theta}$	Platform velocities V_{PG}

A. Choice of Inputs $\dot{\theta}$

Following [4], we group the platform/ground relative velocities V_{PG} and contact velocities $\tilde{V}_c$ together in $V_{GC} = \begin{bmatrix} V_{PG}^T & \tilde{V}_c^T \end{bmatrix}^T$. Jacobian matrices can be formed such that:

$$J_{GC}\ V_{GC} = J_R\ \dot{\theta}. \tag{6}$$

Equations (6) are constraints which relate the joint velocities $\dot{\theta}$ to the relative ground/platform and contact velocities V_{GC}. In the general case neither J_{GC} nor J_R are square and thus are not invertible.

Because of the constraints (6) we cannot freely choose our inputs $\dot{\theta}$. However, we can calculate inputs consistent with

(6) which are as close as possible (in the least-squares sense) to a vector of desired inputs. This is done as follows. Let c be the number of columns of J_{GC}. The QR decomposition [7] of matrix J_{GC} is:

$$J_{GC} = Q\,R.$$

Let $r = rank(J_{GC})$. Split Q into $[Q_1\,Q_2]$, where $Q_2 \in \Re^{c\times(c-r)}$. Q_2 forms a orthonormal basis for the null space of J_{GC}^T, meaning $J_{GC}^T\,Q_2 = 0$ or $Q_2^T\,J_{GC} = 0$. Pre-multiplying both sides of 6 by Q_2^T yields:

$$Q_2^T\,J_{GC}\,V_{GC} = Q_2^T\,J_R\,\dot{\theta},$$

or

$$Q_2^T\,J_R\,\dot{\theta} = 0. \tag{7}$$

Equation (7) is a set of constraint equations for the inputs $\dot{\theta}$. To make use of these equations, let $C_\theta = (Q_2^T\,J_R) \in \Re^{p\times q}$ and $rank(C_\theta) = p$. The QR decomposition of C_θ^T is:

$$C_\theta^T = [Q_{C1}\;Q_{C2}]\;R_C,$$

where $Q_{C2} \in \Re^{q\times p}$. Then $C_\theta\,Q_{C2} = 0$, meaning Q_{C2} is an orthonormal basis for the null space of C_θ. At this point, we can choose independent generalized velocity inputs $\dot{\theta}_g$ such that

$$\dot{\theta} = Q_{C2}\,\dot{\theta}_g. \tag{8}$$

However, since neither C_θ nor Q_{C2} are unique and both change as the robot configuration changes, the generalized inputs $\dot{\theta}_g$ have no physical interpretation and their relationship with the actual joint velocities $\dot{\theta}$ is unclear.

Since (8) is of limited use, we take another step. We want our actual joint velocities $\dot{\theta}$ to match some desired joint velocities $\dot{\theta}_d$, or $\dot{\theta} \approx \dot{\theta}_d$. Combining this with (8), we have:

$$Q_{C2}\,\dot{\theta}_g \approx \dot{\theta}_d.$$

To get as close as possible in the least squares sense to $\dot{\theta}_d$, use the pseudo-inverse [12] of Q_{C2}:

$$\dot{\theta}_g = Q_{C2}^+\,\dot{\theta}_d = (Q_{C2}^T Q_{C2})^{-1} Q_{C2}^T\,\dot{\theta}_d. \tag{9}$$

Since the columns of Q_{C2} are orthonormal, Q_{C2}^+ reduces to Q_{C2}^T. Noticing that $\dot{\theta} = Q_{C2}\,\dot{\theta}_g$, we can pre-multiply both sides of (9) by Q_{C2} to get:

$$Q_{C2}\dot{\theta}_g = Q_{C2}Q_{C2}^T\dot{\theta}_d,$$

or

$$\dot{\theta} = Q_{C2}Q_{C2}^T\dot{\theta}_d = J_{in}\dot{\theta}_d. \tag{10}$$

J_{in} can be thought of as a transformation that takes the desired velocities $\dot{\theta}_d$, which can be arbitrary, and transforms them such that $\dot{\theta}$ satisfy the constraints (6) while remaining as close as possible to $\dot{\theta}_d$.

Equation (10) is a highly useful result for our simulation. First, it eliminates the need to deal with independent generalized velocities $\dot{\theta}_g$, which have no physical meaning. We can instead directly specify a desired set of joint velocity inputs $\dot{\theta}_d$ and get a set of actual inputs $\dot{\theta}$ which satisfies the constraints (6) of the robot/ground system. Second, $\dot{\theta}$ is guaranteed to be as close as possible to $\dot{\theta}_d$ in the least squares sense. Third, (10) gives us control over the type of motion we want: for instance, if we want a motion trajectory that minimizes the PVC joint angles $\gamma_{2,3}$ then we set $\dot{\gamma}_{2d} = \dot{\gamma}_{3d} = 0$. The actual γ values will then remain as close to 0 as the system constraints permit.

B. Holonomic Closure Constraints

The robot/ground system is modeled as a hybrid series-parallel mechanism. Each wheel is itself a kinematic chain between the platform and the ground, and there are three such chains in parallel. The *closure constraints* [11] for the parallel mechanism specify that each kinematic chain must end at the same frame (in this case, $\{P\}$). Let T_{AB} be the 4×4 homogeneous rigid body transform between frames A and B. Then the closure constraints for the robot are

$$T_{GP,wheel1} = T_{GP,wheel2} = T_{GP,wheel3}. \tag{11}$$

These can be interpreted as ensuring that the robot platform remains rigid: proper relative lengths and orientations are preserved. Equations (11) can be written as

$$\begin{aligned} T_{GP,wheel1} - T_{GP,wheel2} &= 0 \\ T_{GP,wheel1} - T_{GP,wheel3} &= 0, \end{aligned} \tag{12}$$

which are algebraic equations of the form $C(q) = 0$. To avoid having to solve a mixture of differential and algebraic equations, $C(q)$ is differentiated to obtain:

$$\dot{C}(q) = \frac{\partial C}{\partial q}\,\dot{q} = J(q)\,\dot{q} = 0. \tag{13}$$

C. Forward Kinematics Equations

We now have all of the tools that we need to make a complete set of ordinary differential equations (ODEs) to model the robot/ground system.

Equations (10) relate the desired and actual joint velocities of the system. The rolling contact equations (4) are the non-holonomic system constraints. The holonomic constraints (13) ensure that the wheels remain in the proper position and orientation relative to one another. As all of these ODEs are linear in the velocity terms, they can be collectively written in the form:

$$M(q)\,\dot{q} = f(q) \tag{14}$$

Equations (14) are a complete model of the system, incorporating enforcement of the rolling contact equations. Solving these equations given desired joint velocity inputs $\dot{\theta}_d$ yields the motion of the entire system, including precise information about how the wheels roll over the uneven terrain.

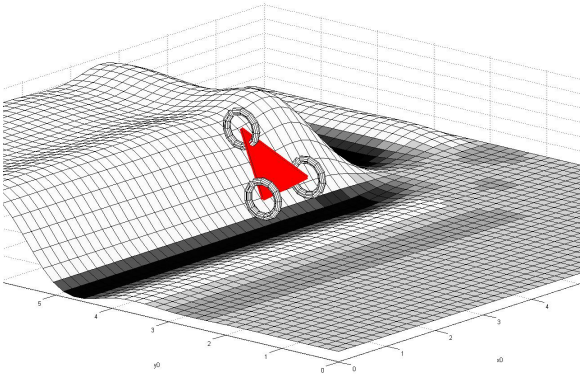

Fig. 4. The wheeled mobile robot on the plateau terrain.

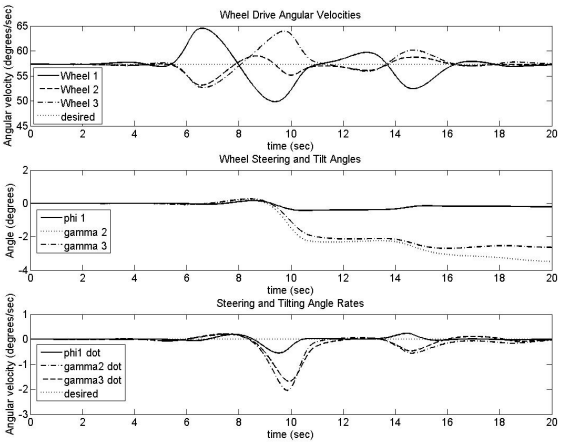

Fig. 5. Joint angles and rates: wheel drive rates, steering angle, and PVC angles.

D. Adaptability of the Modeling Method

Our formulation is adaptable to other vehicle designs of arbitrary complexity: one simply has to create new coordinate transforms T_{GP} which reflect the geometry of the new system. All other equations will remain identical in structure to those presented here. This makes our modeling method versatile and powerful for realistic kinematic simulations of outdoor vehicles operating on rough terrains.

V. Results and Discussion

The kinematic simulation was run on several different surfaces and for various inputs. MATLAB's ODE suite was used to solve (14) and the Spline Toolbox was used to generate the ground surfaces. We present results for two surfaces: a high plateau and a randomly-generated hilly terrain.

A. Climbing a Hill

As a demonstration of the usefulness of our modeling method, here we present a simulation of the 3-wheeled mobile robot climbing a steep hill onto a plateau. To the authors' knowledge, this simulation, which precisely represents the rolling motion of the wheels on a complex ground surface, is not possible with other existing methods. Fig. 4 shows the 3-wheeled robot climbing the hill.

The hill climbing simulation was run for 20 seconds with the following desired inputs:

- Steering rate $\dot{\phi}_1 = 0$
- Driving rates $\dot{\alpha}_{1,2,3} = 1\, rad/sec \approx 57.3\, deg/sec$
- PVC joint rates $\dot{\gamma}_{2,3} = 0$.

Fig. 5 plots the $\dot{\theta}$ inputs and the steering and PVC angles along with their desired values $\dot{\theta}_d$.

B. Random Terrain

Our simulation also works for more general and complex surfaces. Fig. 6 shows the 3-wheeled robot negotiating a randomly-generated ground surface.

The inputs for this simulation were the same as for the hill climbing simulation in the previous section. Fig. 7 plots the paths of the 3 wheel/ground contact points in the ground x-y plane. It also shows the projections of the wheel centers in that plane, to show that the wheels tilt as the robot traverses the uneven terrain. The platform velocities V_p are plotted in fig. 8.

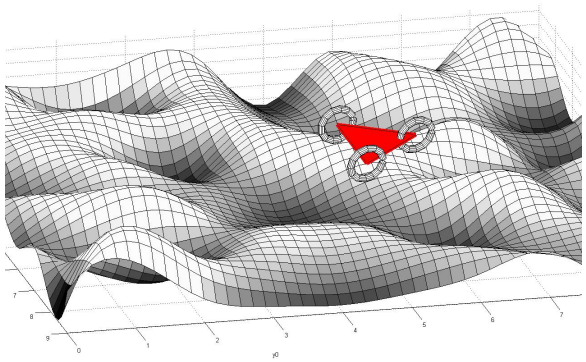

Fig. 6. The wheeled mobile robot on the random terrain.

Fig. 9 plots the L_2 error in satisfaction of the holonomic constraints (12) and the rolling contact kinematic equations (4). Fig. 9 shows that the constraint equations are well satisfied during the course of the simulation. This means that the PVC-equipped vehicle is able to move over the difficult terrain with negligible wheel slip. Had we not used dextrous manipulation kinematics to precisely model the wheel motion, it would not have been possible to verify PVC's performance in this way.

VI. Conclusion and Future Work

In this paper we have presented a novel way of modeling wheeled vehicles on outdoor terrains. In order to precisely model the way that three dimensional wheels roll over uneven terrain, we adapted concepts developed for modeling dextrous robot manipulators. Our method provides a concise and meaningful set of ordinary differential equations which completely describe the kinematics of the robot/ground sys-

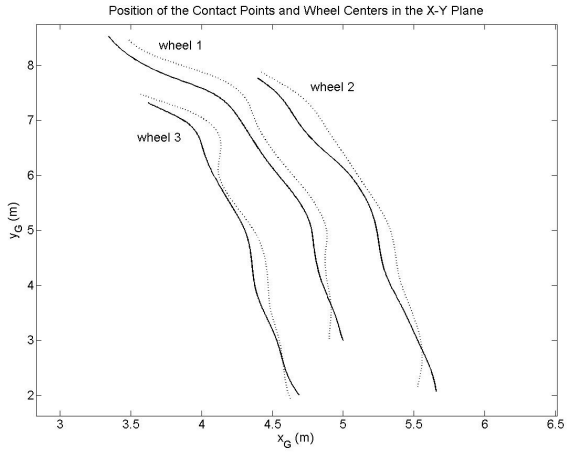

Fig. 7. The wheel/ground contact points (dotted) and wheel centers (solid) in the xG-yG plane.

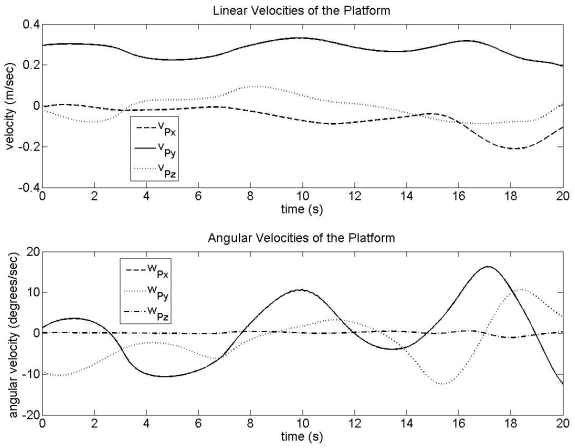

Fig. 8. The platform linear and angular velocities V_p.

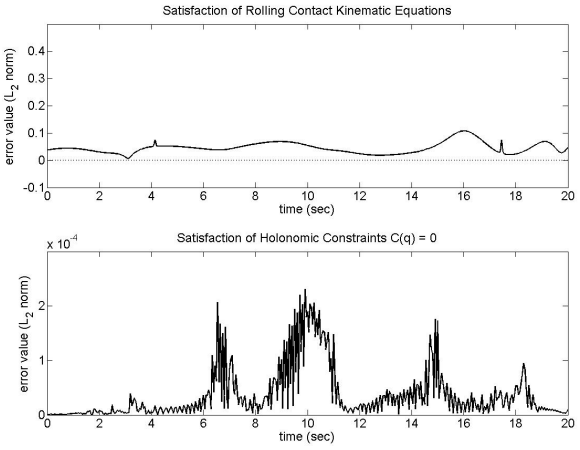

Fig. 9. The L_2 error in satisfaction of the holonomic and non-holonomic constraints.

tem. Also, our method is easily adaptable to other vehicle designs of arbitrary complexity.

The purpose of the simulation is to validate a new concept for design of off-road vehicle wheel suspensions. We used our modeling techniques to simulate the motion of a three-wheeled vehicle with two Passive Variable Camber joints. The results demonstrate that the vehicle can negotiate an extreme terrain without kinematic slip, thus improving vehicle efficiency and performance.

Our next step will be a dynamic simulation of the PVC-equipped robot. This will allow a comparison of dynamic slip and power consumption with and without PVC. We are also designing an experimental set-up by which we can verify that a real wheel and axle with a PVC joint can negotiate an uneven surface with reduced or eliminated kinematic and dynamic slip and less power consumption than a regular wheel/axle combination.

REFERENCES

[1] Alexander, J.C., Maddocks, J.H. 1989. "On the Kinematics of Wheeled Mobile Robots". *The Intl. J. of Robotics Res.*, vol. 8, no. 5, pp. 15-27.

[2] Chakraborty, N., Ghosal, A. 2004. "Kinematics of Wheeled Mobile Robots on Uneven Terrain". *Mech. and Machine Theory*. Vol. 39, no. 12, pp. 1273-1287.

[3] Grand, C., BenAmar, F., Plumet, F., and Bidaud, P. 2004. "Decoupled Control of Posture and Trajectory of the Hybrid Wheel-Legged Robot Hylos". *Proc. 2004 ICRA*.

[4] Han, L., Trinkle, J.C., and Li, Z.X. 1997. "The Instantaneous Kinematics and Planning of Dextrous Manipulation". *Proc. 1997 IEEE Intl. Symp. on Assembly and Task Planning*, pp. 60-65.

[5] Huntsberger, et al. 2002. "Rover Autonomy for Long Range Navigation and Science Data Acquisition on Planetary Surfaces". *Proc. of 2002 IEEE ICRA*.

[6] Iagnemma, K., et al. 2003. "Experimental Study of High-speed Rough-terrain Mobile Robot Models for Reactive Behaviors". *Springer Tracts in Advanced Robotics*. Vol. 5, pp. 654-663.

[7] Kim, S.S., and Vanderploeg, M.J. 1986. "QR Decomposition for State Space Representation of Constrained Mechanical Dynamic Systems". *J. of Mech., Trans., and Automation in Design*, Vol. 108, pp. 183-188.

[8] Laulusa, A., and Bauchau, O. A. 2007. "Review of Classical Approaches for Constraint Enforcement in Multibody Systems". *J. of Computational and Nonlinear Dynamics*, submitted for publication.

[9] Meghdari, A., et al. 2004. "Dynamics Modeling of "Cedra" Rescue Robot on Uneven Terrains". *Proc. of IMECE2004*.

[10] Montana, D. 1988. "The Kinematics of Contact and Grasp". *The International Journal of Robotics Research*, Vol. 7, No. 3, pp. 17-32.

[11] Murray, R., Li, Z., and Sastry, S. 1994. *A Mathematical Introduction to Robotic Manipulation.* CRC Press: Boca Raton.

[12] Nash, J.C. *Compact Numerical Methods for Computers*. Second Edition. Adam Hilger Publishing, Bristol. 1990.

[13] Sreenivasan, S.V., Nanua, P. 1999. "Kinematic Geometry of Wheeled Vehicle Systems". *Trans. of the ASME J. of Mech. Des.*, Vol. 121.

[14] Tai, M. 2003. "Modeling of Wheeled Mobile Robot on Rough Terrain". *Proc. of IMECE2003*.

[15] Tarokh, M., McDermott, G., Hiyati, S., and Hung, J. 1999. "Kinematic Modeling of a High Mobility Mars Rover". *Proc. of 1999 ICRA*.

[16] Waldron, K. 1994. "Terrain Adaptive Vehicles". *ASME Journal of Mech Des*. Vol 117, pp. 107-112.